

# New Materials for Optical Rectification and Electrooptic Sampling of Ultrashort Pulses in the Terahertz Regime

L. MICHAEL HAYDEN<sup>1</sup>, ALEXANDER M. SINYUKOV<sup>1</sup>, MEGAN R. LEAHY<sup>1</sup>, JOEY FRENCH<sup>1</sup>, PETER LINDAHL<sup>1</sup>, WARREN N. HERMAN<sup>2</sup>, ROBERT J. TWIEG<sup>3</sup>, MENG HE<sup>3</sup>

<sup>1</sup>Department of Physics, University of Maryland Baltimore County, Baltimore, Maryland 21250

<sup>2</sup>Laboratory for Physical Sciences, College Park, Maryland 20740

<sup>3</sup>Department of Chemistry, Kent State University, Kent, Ohio 44242

Received 27 January 2003; revised 4 March 2003; accepted 4 March 2003

**ABSTRACT:** The synthesis and nonlinear optical characterization of new electrooptic (EO) materials useful for terahertz (THz) applications is presented. Semiempirical calculations were used to guide the development of a series of chromophores on the basis of 2-dicyanomethylen-3-cyano-4,5,5-trimethyl-2,5-dihydrofuran acceptors acting as guests in polymer films used in the generation of THz radiation via optical rectification. Amorphous films, 65–250  $\mu\text{m}$  thick, with EO coefficients as high as 52 pm/V at 785 nm were used to generate sub-picosecond pulses with bandwidths up to 3 THz.

© 2003 Wiley Periodicals, Inc. *J Polym Sci Part B: Polym Phys* 41: 2492–2500, 2003

**Keywords:** optics; nonlinear polymers; host-guest systems

## INTRODUCTION

An organic electrooptic medium can be designed and built in a variety of ways as defined by the identities and relationships of the components. In the case of polymeric electrooptic media, the physical connectivity of the molecular components results in a variety of possible configurations.<sup>1,2</sup> The guest–host configuration is often used early in a development cycle to obtain a polymer electrooptic material suitable for preliminary device building. In the guest–host configuration, an active guest electrooptic nonlinear optical (NLO) chromophore is physically blended with a passive and easily processed host polymer. Although this approach may not ultimately deliver all of the physical properties required in an application, such as

the temporal stability of poled order, it does offer the greatest ease in the design and availability of the components. The guest NLO chromophore can be chosen from a wide array of known systems with a range of established physical properties such as absorption spectra ( $\lambda_{\text{max}}$  and cutoff), dipole moments (ground-state  $\mu_{\text{g}}$  and excited-state  $\mu_{\text{e}}$ ), and the second-order molecular optical polarizability (the frequency-dependent  $\beta$ ). Alternatively, known chromophores might be custom-modified to fit the application, or even entirely new chromophore classes can be investigated. Likewise, a well-established group of glass-forming polymers now exists with suitable physical properties that may be selected as the host. The polymer is chosen on the basis of its rheological properties including its glass-transition temperature ( $T_{\text{g}}$ ) and capabilities for processing into thin films. The dielectric and linear optical properties of the polymer, including transparency at appropriate wavelengths, are also very important.

Correspondence to: L. M. Hayden (E-mail: hayden@umbc.edu)

*Journal of Polymer Science: Part B: Polymer Physics*, Vol. 41, 2492–2500 (2003)  
© 2003 Wiley Periodicals, Inc.

Although the individual physical properties of both chromophore guest and polymer host play a dominant role in dictating device fabrication and performance parameters, their interactions and compatibility must also be considered. The chromophore and polymer must be physically compatible so that a sufficient amount (typically  $30 \pm 20$  wt %) of the chromophore can be added to the polymer to achieve the desired bulk electrooptic coefficient without the occurrence of phase separation. The added chromophore usually behaves as a plasticizer for the polymer. The intrinsic  $T_g$  of the polymer must be large enough so that the glass transition of the composite ends up in a useful range for poling and stability. The stability issue falls into two different categories. First, the poled-order stability, related to the difference between the poling temperature to create the active device and the operation temperature of the device, must be maximized. Second, the thermochemical stability of the chromophore (or possibly, but less likely, the polymer) may dictate an upper bound on the poling temperature.<sup>3</sup> The poling temperature is usually at or below the glass transition of the polymer–chromophore composite.

In addition to the morphological properties that are influenced by blending polymer and chromophore, there is also a comparable and important set of electronic and optical properties influenced by their mixing. For guided wave applications, the index of the media must be considered and matched with that of a confinement medium. Because electrooptic NLO chromophores are often highly solvatochromic, the host media may influence the important molecular properties including both the absorption and optical hyperpolarizability. In addition, because of their highly polar nature, NLO chromophores have a propensity to dimerize, leading to a lower order parameter and a concomitant decrease in macroscopic nonlinearity. The chromophore identity and concentration as well as the host identity will all influence the extent of aggregation of the chromophore molecules as well as the loading level tolerated short of phase separation.

This work describes the adaptation of electrooptic polymer technology to terahertz (THz) generation and detection<sup>4</sup> and involves both the adoption of established materials as well as their tailoring and the development of new materials. The generation of wide-bandwidth THz radiation (mid IR and far IR) with a smooth frequency response with low power laser sources would be

quite valuable in many scientific and technological arenas. The driving force behind the work presented here is the wealth of applications and technologies that could be addressed if better emitters and detectors of wideband THz radiation could be produced. Electrooptic (EO) polymers have the potential to make a significant impact in this field. Some of the varied applications of THz radiation now under investigation include IR measurements of the water content in living plants, trace gas analysis, flame emissions, quality control of plastic parts, burn-depth assessments, and semiconductor wafer characterization;<sup>5</sup> imaging and analysis of dental caries, periodontal disease, and skin cancer;<sup>6</sup> and vibrational analysis of biomolecules.<sup>7–10</sup>

## MATERIALS

Among the many options available as the polymer hosts, both an acrylate polymer poly(methyl methacrylate) (PMMA) and a polycarbonate copolymer (APC, the bisphenol comonomers were derived from acetone and 3,3,5-trimethylcyclohexanone) were evaluated. Of course, PMMA has enjoyed ubiquitous utility in the NLO area for a long time both as a host polymer and as a copolymer into which the active NLO chromophore is covalently introduced. APC is a commercially available polycarbonate that has been used in our previous studies as well as in other electrooptic systems.<sup>11</sup> APC forms high-quality spin-coated films and has reasonable compatibility with many chromophores. The intrinsic  $T_g$  of this polymer is 205 °C and is sufficiently high to permit the addition of an adequate host chromophore and still retain a useful  $T_g$  ensuring useful poled-order temporal stability for the composite.

Just as in the case of the polymer hosts, there are also numerous options available when it comes to a choice of the NLO chromophore. NLO chromophores are characterized by three important structure features: (1) an electron-rich donor group (usually an amine and often grouped with an aromatic ring, such as an aniline derivative); (2) a group of additional  $\pi$ -conjugated ring(s), alkene(s), azo linkages, and the like; and (3) an electron-deficient group (usually containing hetero atoms in high oxidation states and sometimes grouped with additional alkene content). The exact identity and combination of these three structure features influence the balance of electronic properties that dictate the chromophores utility

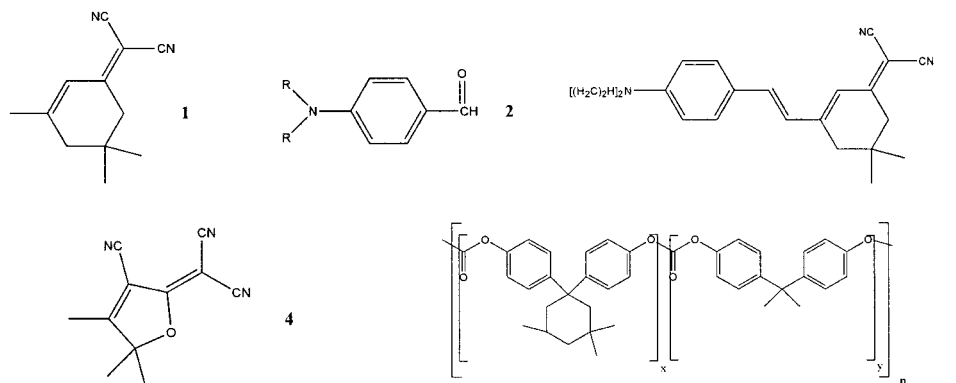


**Figure 1.** The **1** characteristic of the Lemke chromophores, a general **2**, Lemke chromophore **3**, the **4** characteristic of the DCDHF chromophores, and the host APC polymer poly[bisphenol A carbonate-co-4,4'-(3,3,5-trimethylcyclohexylidene)diphenol carbonate].

in a particular application. For example, as the strength of the donor–acceptor combination and/or the length and identity of the conjugated pathway is tuned, the linear and nonlinear polarizabilities used in a given application vary in a systematic fashion.<sup>12,13</sup> The THz experiments described here have utilized two general classes of dyes that differ primarily in the identity of the acceptor portion of the molecules. The initial experiments were performed with the 2-[3-[2-(4-dialkylaminophenyl)vinyl]-5,5-dimethylcyclohex-2-enylidene]malononitrile dyes (otherwise designated as “Lemke dyes” after the researcher who originally described their synthesis).<sup>14</sup> The acceptor group derived from (3,5,5-trimethylcyclohex-2-enylidene)-malononitrile (**1**) characterizes the Lemke dyes. This unit is condensed at the activated 3-methyl group with a dialkylamine-substituted aromatic aldehyde (**2**) to create the olefinic linkage found in the complete Lemke dye (**3**). These Lemke dyes have also found prior application in EO<sup>15,16</sup> as well as in photorefractive media.<sup>17–19</sup> The subsequent group of experiments involves dyes that contained a different acceptor unit derived from 2-dicyanomethylen-3-cyano-4,5,5-trimethyl-2,5-dihydrofuran (**4**). This heterocycle was first synthesized by a CNRS group in 1995 that also demonstrated its condensation at the active 4-methyl group with aromatic aldehydes.<sup>20</sup> With aromatic aldehydes **2** more typical of NLO molecules, these systems were modified and subsequently exploited effectively as EO chromophores especially including cases where there is substantial conjugation (thiophene and polyolefin) connectivity introduced between the amine donor-substituted ring

unit and the acceptor unit.<sup>1,21–23</sup> The structures of some of the chromophores and intermediates discussed thus far are found in Figure 1.

Although the specific chromophore CLD-1 **5j** (containing tetraene connectivity) has been successfully used for EOs,<sup>23</sup> the preliminary attempted applications of this chromophore for THz experiments were frustrated by crystallization of the dye at a 25% loading level in APC and absorptive losses because of incompatibility with 800-nm lasers used in the study. The crystallization is only seen in the thick (>100  $\mu\text{m}$ ) films required for efficient THz generation. No crystallization was observed in films  $\sim 2 \mu\text{m}$  thick. Subsequently, a number of smaller and less conjugated versions of these dyes have become available because of their efficacy as chromophores in both composite and monolithic photorefractive applications.<sup>24,25</sup> In these cases, the chromophores are named as “DCDHF” systems after the acceptor unit. Very recently, these DCDHF chromophores have been demonstrated to perform effectively in near-infrared photorefractive applications,<sup>26</sup> have been found to possess novel single-molecule fluorescence properties,<sup>27</sup> and are involved in the first demonstration of optical solitons in a polymer photorefractive medium.<sup>28</sup> Structure modification and applications of the DCDHF chromophores as EO media for THz detection and generation comprise the remainder of this discussion. The structures of DCDHF chromophores under study are found in Figure 2.

DCDHF chromophores are particularly useful for a variety of reasons ranging from flexibility in the preparative chemistry and physical properties to their generally impressive thermal stabil-

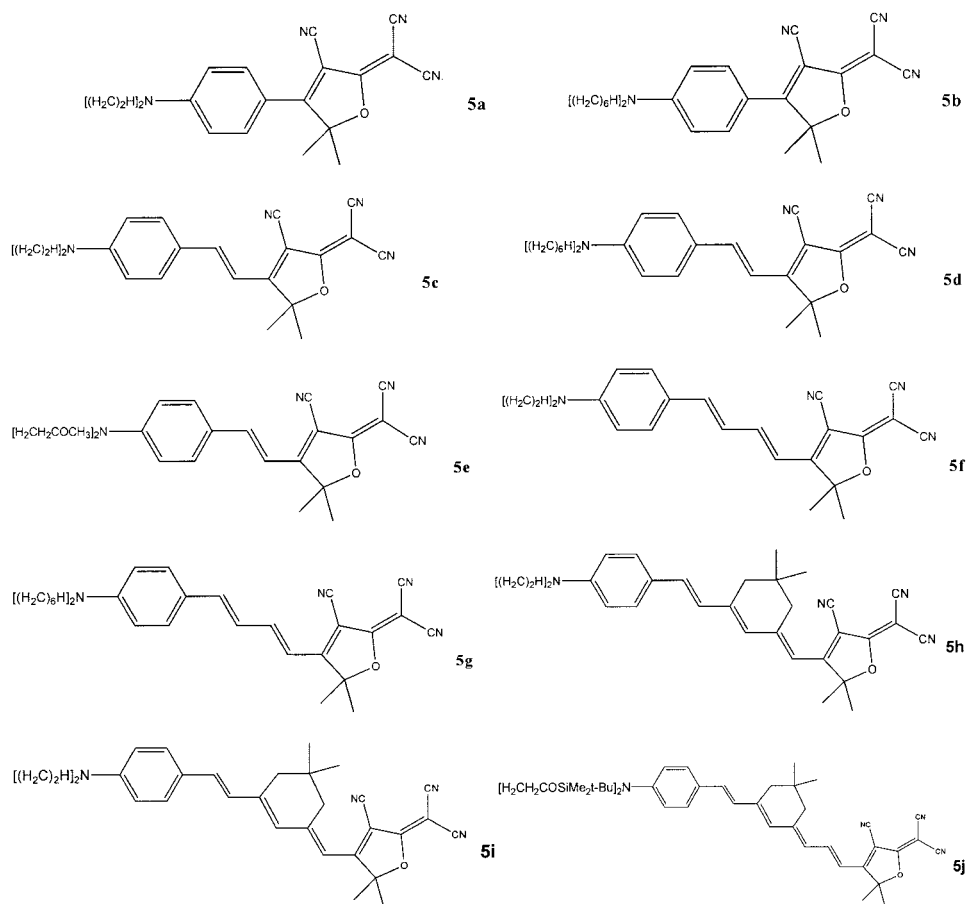


**Figure 2.** DCDHF-2 **5a**, DCDHF-6 **5b**, DCDHF-2-V **5c**, DCDHF-6-V **5d**, DCDHF-MOE-V **5e**, DCDHF-2-2V **5f**, DCDHF-6-2V **5g**, DCDHF-2-3IV **5h**, DCDHF-6-3IV **5i**, and CLD-1 **5j**.

ity. Heterocycle precursor **4** is itself prepared from condensation of two molecules of malononitrile with the  $\alpha$ -disubstituted  $\alpha$ -hydroxyketone 3-methyl-3-hydroxy-2-butanone. DCDHF dyes such as DCDHF-2 **5a** and DCDHF-6 **5b** with no alkene connection require the synthesis of custom  $\alpha$ -hydroxyketones. The other alkene-containing DCDHF dyes examined, DCDHF-2V **5c**, DCDHF-MOE-V **5e**, and DCDHF-6-V **5d**, are prepared by condensation of the appropriate aldehyde with **4**. These latter three chromophores differ only in the amine substituents that have a minor influence on the electronic properties such as absorption and nonlinearity but a significant influence on the melting point and miscibility with the host polymer. The addition of conjugation between the donor–acceptor sections leads to enhancement in the desired properties of dipole moment and nonlinearity but at the expense of longer wavelength absorption and generally a compromise in solubil-

ity. Some of the important physical properties of the dyes examined here are found in Table 1.

DCDHF chromophores with a single alkene connector outperform the comparable Lemke dyes in this application. We are now evaluating DCDHF chromophores with diene (DCDHF-2-2-V **5f** and DCDHF-6-2-V **5g**) and triene (DCDHF-2-3-IV **5h** and DCDHF-6-3-IV **5i**) connectivity to examine the structure trade-offs with performance.

## EXPERIMENTAL

All of the films used in this study were guest–host mixtures in maximum concentrations determined by the solubility of a given chromophore in the APC host. The Lemke dye was obtained from Chromophore, Inc. CLD-1 was obtained from the laboratory of C. Zhang and L. R. Dalton. APC was

**Table 1.** Chromophore Properties

Chromophore	$ \beta  \cos \theta$ ( $\text{Cm}^3/\text{V}^2$ ) $\times 10^{-49}$	$ \mu $ (Cm) $\times 10^{-29}$	MW (kg/mol)	EO FOM ( $\mu\cdot\beta/\text{M}$ ) $\times 10^{-77}$	FOM w.r.t. Lemke	$\lambda_{\text{max}}$ (nm)	$r_{33}$ (pm/V) at 80 V/ $\mu\text{m}$ (Maximum $r_{33}$ )	Maximum Loading (%)
DCDHF-6	1.6	4.1	0.445	1.4	0.9	483	—	—
DCDHF-6-3IV	2.3	3.8	0.591	1.5	0.9	—	—	—
Lemke	2.0	2.8	0.345	1.6	1.0	512	27 (51)	40
DCDHF-2	1.4	4.0	0.332	1.7	1.1	480	10 (10)	30
CLD-1	5.2	3.6	0.765	2.5	1.6	667	—	< 25
DCDHF-2-3IV	3.1	4.1	0.479	2.6	1.7	—	—	—
DCDHF-6-V	3.4	4.3	0.471	3.1	1.9	568	45 (52)	40
DCDHF-MOE-V	3.2	4.0	0.418	3.1	2.0	530	21 (21)	25
DCDHF-2-V	3.1	4.2	0.358	3.7	2.3	542	—	< 10
DCDHF-6-2V	5.0	4.4	0.497	4.4	2.8	—	—	—
DCDHF-6-V/MOE-V						562	38 (43)	Mixture; 20% each

The first four columns are results from MOPAC calculations, and the remaining columns are experimental results. The EO coefficient  $r_{33}$  at a poling field of 80 V/ $\mu\text{m}$  is reported for each system (maximum  $r_{33}$  value obtained to date in parentheses).

obtained from Aldrich Chemical Co. The films were made by dissolving each component in dichloroethane in a 10% solids/solvent ratio and spreading the solution on indium tin oxide (ITO) coated glass slides to allow the solvent to evaporate. The films were then further baked at  $T_g$  to completely remove the solvent. After baking, a sandwich was made of two polymer-coated slides by pressing the slides together in a vacuum oven at  $\sim 170^\circ\text{C}$  for 10 min. Spacers of polyimide sheet were placed between the slides to control the film thickness. Films about 50–250  $\mu\text{m}$  thick can easily be obtained in this fashion. A nonzero EO coefficient was imparted to the film by application of an electric field across the ITO electrodes in the sandwich while the sample temperature was held above the  $T_g$  of the composite. After cooling the films to room temperature, the EO coefficients were measured with the ellipsometric method.<sup>29</sup> Because the ITO coatings are conductive, they have very low transmittance in the THz regime and act like mirrors for the generated THz radiation. With the polymers in the THz setup, one of the ITO slides was removed from the sandwich to allow the generated THz radiation to propagate unimpeded. The film remained on one of the slides and was placed in the optical beam so that the THz beam did not transit the remaining ITO layer. When used in this fashion, we saw no change in the THz signals emitted or detected by

the polymer films as compared with the situation where we removed the polymer film from the substrate completely to create a free-standing film. The index of refraction (3–5  $\mu\text{m}$  thick films) was measured with the prism-coupling technique.<sup>30</sup> Semiempirical calculations were performed on each chromophore with MOPAC6 [AM1, PRECISE, Eigenvector Following, POLAR (Pockels Effect)] to obtain the ground-state dipole moment ( $\mu$ ) and the first hyperpolarizability ( $\beta$ ).

We used a standard arrangement<sup>31</sup> for generating and detecting the free-space propagation of THz waves (Fig. 3). The laser was a regeneratively amplified Ti:Sapphire (Coherent Mira/RegA 9000) that supplied  $\sim 180$  fs, 3–4  $\mu\text{J}$ , and 800-nm optical pulses at 250 kHz. For the comparisons between the EO polymers and the ZnTe as THz emitters, 90 mW of laser power were focused to an elliptical spot of  $6 \times 10^{-4}$   $\text{cm}^2$  (150 W/ $\text{cm}^2$ ). The ZnTe crystal was illuminated by  $p$ -polarized light at normal incidence with the crystal rotated about the surface normal by  $55^\circ$  with respect to the  $\langle 110 \rangle$  direction to maximize the THz output.<sup>32</sup> The polymer films were illuminated at an incident angle of  $55^\circ$  with  $p$ -polarized light. The detection was performed with crossed-polarizers. For the ZnTe case, the normally incident probe beam was  $p$ -polarized, and the crystal was rotated about the  $\langle 110 \rangle$  direction to maximize the detected signal. For the polymer case, the probe

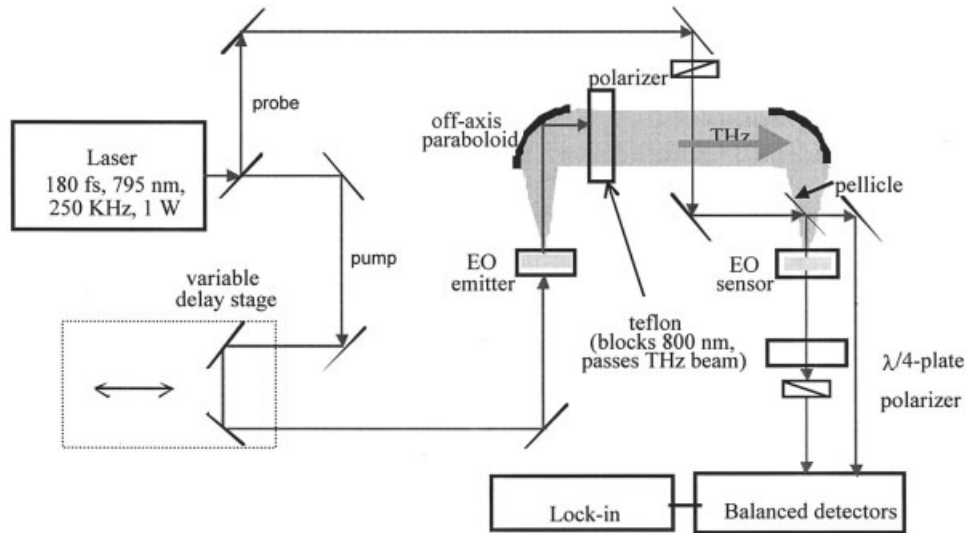


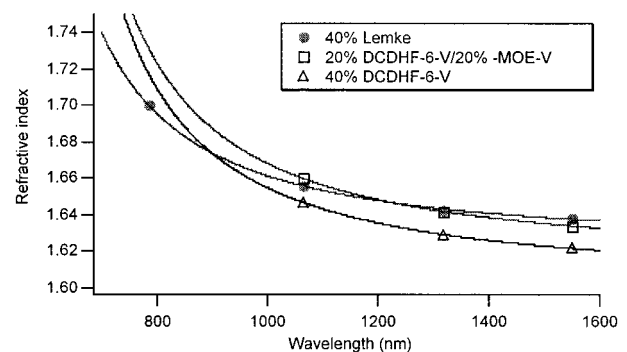
**Figure 3.** Experimental setup for generation and detection of THz radiation. The 180 fs pump laser is incident on the EO emitter generating a THz pulse via optical rectification. The THz pulse propagates to the EO sensor inducing a change in the refractive index of the sensor via the electrooptic effect. The polarization of the probe beam is modified by the changing refractive index in the sensor and detected via a crossed-polarizer arrangement and a balanced photodetector pair.

beam was incident to the polymer at  $55^\circ$  and was polarized at  $45^\circ$  with respect to the plane of incidence to maximize the overlap of the probe-beam polarization with the NLO coefficients of the poled polymer because the  $c$  axis of the poled polymer is normal to the surface of the film for the sandwich poling geometry.

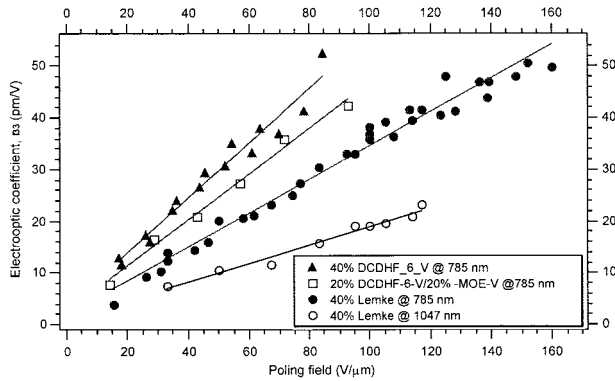
## RESULTS AND DISCUSSION

Figure 4 displays the results of the prism-coupling measurements of the index of refraction of three of the most useful composites examined. These data are important to the development of EO polymers to be used as emitters of THz radiation. We used optical rectification<sup>33</sup> (OR) to generate the THz radiation. When an intense optical beam is incident on a second-order NLO medium, a direct current (dc) polarization can be generated through the process of OR. Because we used short optical pulses to pump the EO polymers, OR occurred only during the duration of the incident pulse, and hence the dc polarization rose and fell on the timescale of the optical pulse width ( $\sim$ fs). This time-dependent change in the polarization of the medium resulted in the emission of an electromagnetic wave. The frequency (THz) bandwidth of the emitted wave depends on the band-

width of the incident optical pulse and the dispersion in the nonlinear medium. OR is a phase-matched process that occurs more efficiently in materials with longer coherence lengths (the length in which the optical pump beam and THz beams overlap inphase). To optimize the coherence length, one needs to match the speed of the optical pulse (optical group velocity) with the speed of the generated THz wave (THz phase velocity). For a given material, we can determine the optical group velocity at any wavelength by



**Figure 4.** The refractive index of three composites. Each composite consists of 40% total chromophore concentration and 60% APC. The curves are best fits of the data to the Sellmeier expression,  $n^2 = A + B\lambda^2/(\lambda^2 - \lambda_{\max}^2)$ .



**Figure 5.** EO coefficient of 40% Lemke/60% APC, 40% DCDHF-6-V/60% APC, and 20% DCDHF-6-V/20% DCDHF-MOE-V/60% APC as a function of poling field. All films were between 65 and 150  $\mu\text{m}$  thick.

taking the derivative of one of the curves in Figure 4.

The coherence length for a dispersive material generating THz waves is given by,

$$l_c = \pi/\Delta k = \pi/[\omega_{\text{THz}}|n_{\text{opt}} - \lambda_{\text{opt}}(dn_{\text{opt}}/d\lambda)_{\lambda_{\text{opt}}} - n_{\text{THz}}|], \quad (1)$$

where  $n_{\text{opt}}$  and  $n_{\text{THz}}$  are the indices associated with the phase velocity.<sup>34</sup> With this equation, we estimated that our composites have coherence lengths of  $l_c \sim 5$  mm at 1 THz. ZnTe and DAST (organic crystal) have coherence lengths of  $l_c \sim 460$  and  $410$   $\mu\text{m}$  at 1 THz, respectively. Including the effects of dispersion raises the coherence lengths of ZnTe and DAST to  $\sim 3$  mm and  $500$   $\mu\text{m}$  at 1 THz, respectively, because of resonances in the phonon bands of each of these crystals in the far IR. At 10 THz the polymer coherence length is expected to still be at least  $500$   $\mu\text{m}$ , whereas at 10 THz the coherence lengths for ZnTe and DAST are  $13^34$  and  $<100$   $\mu\text{m}$ ,<sup>35</sup> respectively. The result of these effects of increased coherence length and EO coefficient ( $r_{33} \sim 50$  pm/V) is that the EO polymers should generate THz fields about three orders of magnitude times that of ZnTe at 10 THz.

In addition to trying to maximize the THz output by controlling the index of refraction, we also need to be concerned with the possible absorption of the pump beam. Our setup now is limited to 800-nm pump beams, and this, for the time being, precludes investigations of many promising EO chromophores with longer conjugation lengths and longer wavelength absorption.

One of the advantages of EO polymers rather than EO inorganic crystals is that the dispersion is much lower from the optical to the THz regime in polymers. This allows for longer coherence lengths (as mentioned previously) and, for a given interaction length, wider THz emission bandwidths. Another advantage of EO polymers over EO crystals (including organic crystals) is that the phonon band structure present in all crystals usually causes significant absorptive losses (gaps) in the THz spectra. For a wide, flat frequency response in the THz regime, EO polymers are very promising because of their amorphous structure. Recently, a smooth 30-THz bandwidth was demonstrated with a copolymer of 2-*N*-[4-(4-nitrophenylazo) indolino] ethyl methacrylate and methyl methacrylate.<sup>36</sup> To help guide our synthetic efforts and to compare with the experimental EO measurements, we calculated the  $\mu$  and the  $\beta$  for each chromophore. Table 1 lists the results of those calculations along with the experimentally determined values of the EO coefficient. Figure 5 exhibits representative plots of the EO coefficient as a function of poling field for three of the composites.

A comparison of the EO figure of merit (FOM) with the experimentally determined  $r_{33}$  values at  $80$  V/ $\mu\text{m}$  shows that the DCDHF chromophores perform better than the Lemke chromophore. However, the experimentally determined values of  $r_{33}$  are about 10% lower than what one would expect from the FOM predictions on the basis of the semiempirical calculations. This is a possible indication that the DCDHF chromophores, with their larger dipole moments, are experiencing the well-known saturation effect<sup>37</sup> because of dipole-dipole interactions. The FOM for DCDHF-MOE-V

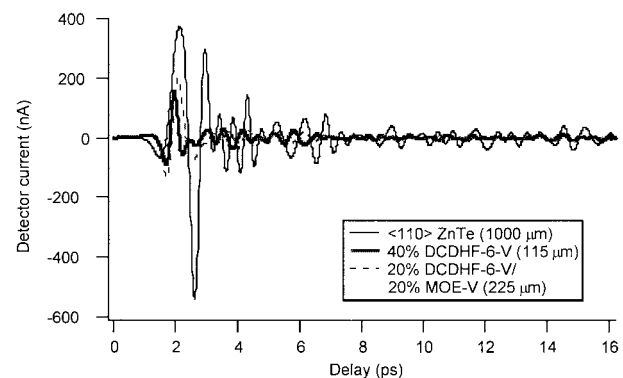


**Figure 6.** Comparison of the relative amplitude of the THz electric field emitted from a ZnTe crystal and from two different EO polymer films.

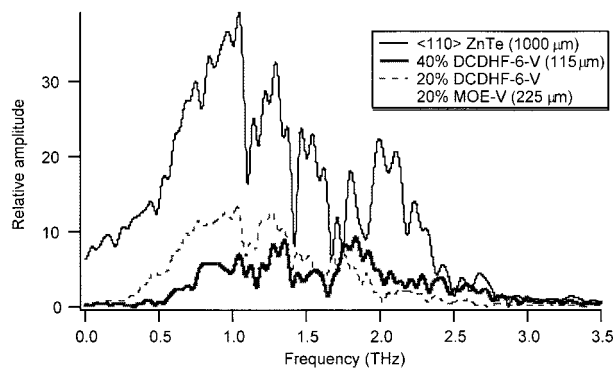


**Figure 7.** Comparison of the THz frequency response corresponding to the THz pulses previously shown in Figure 6. Several absorption features (e.g.,  $\sim 1.1$ ,  $1.4$ ,  $1.7$ , and  $1.9$  THz) are visible that are due to water vapor in the THz beam path. The limited bandwidth for all the traces ( $\sim 2.5$  THz) is the result of a thick (2-mm) ZnTe crystal as the THz sensor.

**5e** was promising, but we could only load APC to 25% before significant crystallization occurred. By mixing **5e** and **5d** we were able to achieve a total loading of 40% without crystallization. However, the mixture did not perform as well as **5d** alone. All of the DCDHF chromophores with diethylamino donors proved to be too insoluble to be of practical value, in contrast to the diethylamino Lemke molecule **3** that is soluble in concentrations up to 40% in APC, perhaps because of its smaller dipole moment. We are looking at other DCDHF chromophores with modifications in the  $\pi$  system and other substituents. In addition, we are now conducting concentration-dependent studies to determine the optimum concentration for DCDHF-6-V **5d** and the DCDHF-6-V/MOE-V mixture.

Figure 6 compares the amplitude of the electric field of a THz pulse emitted from a ZnTe crystal and two of the DCDHF composites. ZnTe is the popular standard for emission of THz radiation via OR. It is also the standard material for use as a sensor of THz radiation with the EO effect.<sup>38</sup> Because ZnTe is so widely used, any new material or process that is proposed to replace ZnTe in this application should be directly compared with it. Figures 6 and 7 demonstrate that the THz emission and attendant far-IR spectral response from the EO polymer composites are within a factor of three of that from the ZnTe crystal, yet are approximately five to eight times thinner.

We have previously shown<sup>4</sup> that the THz emission from EO polymers scales linearly with the

thickness of the polymer film. Additional improvements are expected with better chromophores and processing. The poling geometry now requires that the optical pump beam be incident on the polymer film at  $\sim 55^\circ$  to ensure efficient overlap of the incident beam electric field with the nonlinear tensor components of the poled film. With films that are poled inplane, we expect an increase in the THz output by a factor of two. In addition, because the composites have nonzero absorption at the pumping wavelength of 800 nm, additional improvements are expected as we migrate to a 1300-nm optical pump. Moreover, as we move to longer pump wavelengths, we will be able to use materials with much larger EO coefficients.<sup>2,39</sup>

## CONCLUSIONS

We have reported the results of our recent work on the development of EO chromophores and their application to the generation of THz electromagnetic radiation via OR. These materials are also capable of sensing the ultrashort THz pulses via the EO effect.<sup>4</sup> The application of semiempirical calculations guides our materials development, and the FOM derived from those calculations is a good predictor of the EO activity of a new composite. Also, the EO coefficient is a good predictor of the relative ability of a given material to produce and detect THz radiation. Because applications in THz radiation range from nondestructive package inspection, protein-folding studies, and ultrafast conductivity studies of materials to biological and chemical weapons detection, efficient, cheap, and compact sources and sensors are needed. Practical implementation of THz technologies may require the use of compact fiber lasers that operate at 1.0, 1.3, or 1.5  $\mu\text{m}$ . THz EO emitters and sensors based on inorganic crystals will not work efficiently in those wavelength ranges. However, EO polymers have already been shown to exhibit large EO coefficients in that range of IR. We believe that further adaptation and optimization of EO polymers for THz applications is promising. Our demonstration of  $>100 \mu\text{m}$  thick films with EO coefficients  $>50 \text{ pm/V}$  is the first step toward achieving those goals. Additional work will be necessary to characterize OR in these materials at 1.0, 1.3, and 1.5  $\mu\text{m}$ .

L. Michael Hayden thanks Larry Dalton for supplying the CLD-1 and the University of Washington for partial

support of this work. This material is based on work supported by the National Science Foundation (ECS-0139457). Robert J. Twieg acknowledges the support of DCDHF chromophore studies by the Air Force Office of Scientific Research (Grant F49620-00-1-0038).

## REFERENCES AND NOTES

- Dalton, L. R.; Steier, W. H.; Robinson, B. H.; Zhang, C.; Ren, A.; Garner, S.; Chen, A.; Londergran, T.; Irwin, L.; Carlson, B.; Fifield, L.; Phelan, G.; Kincaid, C.; Amend, J.; Jen, A. *J Mater Chem* 1999, 9, 1905–1920.
- Ma, H.; Liu, S.; Luo, J.; Suresh, S.; Liu, L.; Kang, S. H.; Haller, M.; Sassa, T.; Dalton, L. R.; Jen, A. K. Y. *Adv Funct Mater* 2002, 12, 565–574.
- Prime, R. B.; Chiou, G. Y.; Twieg, R. J. *J Therm Anal* 1996, 46, 1133–1150.
- Sinyukov, A. M.; Hayden, L. M. *Opt Lett* 2002, 27, 55–57.
- Mittleman, D.; Jacobsen, R. H.; Nuss, M. *IEEE J Quantum Electron* 1996, 2, 679.
- Fitzgerald, A. J.; Berry, E.; Zinovev, N. N.; Walker, G. C.; Smith, M. A.; Chamberlain, J. M. *Phys Med Biol* 2002, 47, 67–84.
- Markelz, A. G.; Roitberg, A.; Heilweil, E. J. *Chem Phys Lett* 2000, 320, 42–48.
- Walther, M.; Plochocka, P.; Fischer, B.; Helm, H.; Jepsen, P. U. *Biopolymers* 2002, 67, 310–313.
- Walther, M.; Fischer, B.; Schall, M.; Helm, H.; Jepsen, P. U. *Chem Phys Lett* 2000, 332, 389–395.
- Fischer, B.; Walther, M.; Jepsen, P. U. *Phys Med Biol* 2002, 47, 3807–3814.
- Ermer, S.; Lovejoy, S. M.; Bedworth, P. V.; Leung, D. S.; Warren, H. B.; Epstein, J. A.; Girton, D. G.; Dries, L. S.; Taylor, R. E.; Barto, R. R.; Eades, W.; Van Eck, T. E.; Moss, A. S.; Anderson, W. W. *Adv Funct Mater* 2002, 12, 605–610.
- Marder, S. R.; Beratan, D. N.; Cheng, L. T. *Science* 1991, 252, 103.
- Marder, S. R.; Cheng, L.-T.; Tiemann, B. G.; Friedli, A. C.; Blanchard-Desce, M.; Perry, J. W.; Skindhøj, J. *Science* 1994, 263, 511.
- Lemke, R. *Synthesis* 1974, 359–361.
- Shu, C.-F.; Tsai, W. J.; Jen, A. K. Y. *Tetrahedron Lett* 1996, 37, 7055–7059.
- Ermer, S.; Lovejoy, S. M.; Leung, D. S.; Warren, H.; Moylan, C. R.; Twieg, R. *J Chem Mater* 1997, 9, 1437–1442.
- Van Steenwinckel, D.; Hendrickx, E.; Persoons, A.; Van den Broeck, K.; Samyn, C. *J Chem Phys* 2000, 112, 11030–11037.
- Strutz, S. J.; Hayden, L. M. *Appl Phys Lett* 1999, 74, 2749–2751.
- Harris, K. D.; Ayachitula, R.; Strutz, S. J.; Hayden, L. M.; Twieg, R. *J Appl Opt* 2000, 40, 2895–2901.
- Melikian, G.; Rouessac, F. P.; Alexandre, C. *Synth Commun* 1995, 25, 3045.
- Zhang, C.; Ren, A. S.; Wang, F.; Zhu, J.; Dalton, L. R.; Woodford, J. N.; Wang, C. H. *Chem Mater* 1999, 11, 1966.
- Zhang, C.; Wang, C.; Yang, J.; Dalton, L. R.; Sun, G.; Zhang, H.; Steier, W. H. *Macromolecules* 2001, 34, 235–243.
- Zhang, C.; Dalton, L. R.; Oh, M. C.; Zhang, H.; Steier, W. H. *Chem Mater* 2001, 13, 3043–3050.
- Wright, D.; Gubler, U.; Roh, Y.; Moerner, W. E.; He, M.; Twieg, R. J. *Appl Phys Lett* 2001, 79, 4274–4276.
- Ostroverkhova, O.; Wright, D.; Gubler, U.; Moerner, W. E.; He, M.; SastreSantos, A.; Twieg, R. J. *Adv Funct Mater* 2002, 12, 621–629.
- Ostroverkhova, O.; Moerner, W. E.; He, M.; Twieg, R. J. *Appl Phys Lett* 2003, 82, 3602–3604.
- Willems, K. A.; Ostroverkhova, O.; He, M.; Twieg, R. J.; Moerner, W. E. *J Am Chem Soc* 2003, 125, 1174–1175.
- Asaro, M.; Chen, Z.; Ostroverkhova, O.; Moerner, W. E.; He, M.; Twieg, R. J.; Salamo, G. *CLEO; Baltimore, MD*, 2003.
- Sandalphon; Kippelen, B.; Meerholz, K.; Peyghambarian, N. *Appl Opt* 1996, 35, 2346–2354.
- Ulrich, R.; Torge, R. *Appl Opt* 1973, 12, 2901.
- Jiang, Z.; Zhang, X. C. *IEEE Trans Microwave Theory Tech* 1999, 47, 2644–2650.
- Chen, Q.; Tani, M.; Jiang, Z.; Zhang, X. C. *JOSA B* 2001, 18, 823–831.
- Zhang, X.-C.; Ma, X. F.; Jin, Y.; Lu, T.-M.; Boden, E. P.; Phelps, P. D.; Stewart, K. R.; Yakymyshyn, C. P. *Appl Phys Lett* 1992, 61, 3080–3082.
- Nahata, A.; Weling, A.; Heinz, T. F. *Appl Phys Lett* 1996, 69, 2321–2323.
- Han, P. Y.; Tani, M.; Pan, F.; Zhang, X.-C. *Opt Lett* 2000, 25, 675–677.
- Cao, H.; Heinz, T. F.; Nahata, A. *Opt Lett* 2002, 27, 775–777.
- Robinson, B. H.; Dalton, L. R. *J Phys Chem A* 2000, 104, 4785–4795.
- Planken, P. C. M.; Nienhuys, H.-K.; Bakker, H. J.; Wenckebach, T. *JOSA B* 2001, 18, 313–317.
- He, M.; Leslie, T. M.; Sinicropi, J. A.; Garner, S. M.; Reed, L. D. *Chem Mater* 2002, 14, 4669–4675.